Toxicology and Applied Pharmacology 280 (2014) 107–116

Contents lists available at ScienceDirect

Toxicology and Applied Pharmacology

journal homepage: www.elsevier.com/locate/ytaap

# Atorvastatin restores arsenic-induced vascular dysfunction in rats: Modulation of nitric oxide signaling and inflammatory mediators

Manickam Kesavan, Thengumpallil Sasindran Sarath, Kandasamy Kannan, Subramaniyam Suresh, Priyanka Gupta, Karunakaran Vijayakaran, Palanisamy Sankar, Nitin Pandurang Kurade, Santosh Kumar Mishra, Souvendra Nath Sarkar *

*Division of Pharmacology and Toxicology, Indian Veterinary Research Institute, Izatnagar, 243122 Bareilly, Uttar Pradesh, India*

ARTICLE INFO

*Article history:*
Received 22 February 2014
Revised 27 June 2014
Accepted 13 July 2014
Available online 21 July 2014

*Keywords:*
Arsenic
Atorvastatin
Vascular dysfunction
Nitric oxide signaling
Inflammatory mediators
Rat

ABSTRACT

We evaluated whether atorvastatin, an extensively prescribed statin for reducing the risks of cardiovascular diseases, can reduce the risk of arsenic-induced vascular dysfunction and inflammation in rats and whether the modulation could be linked to improvement in vascular NO signaling. Rats were exposed to sodium arsenite (100 ppm) through drinking water for 90 consecutive days. Atorvastatin (10 mg/kg bw, orally) was administered once daily during the last 30 days of arsenic exposure. On the 91st day, blood was collected for measuring serum C-reactive protein. Thoracic aorta was isolated for assessing reactivity to phenylephrine, sodium nitroprusside and acetylcholine; evaluating eNOS and iNOS mRNA expression and measuring NO production, while abdominal aorta was used for ELISA of cytokines, chemokine and vascular cell adhesion molecules. Histopathology was done in aortic arches. Arsenic did not alter phenylephrine-elicited contraction. Atorvastatin inhibited $E_{max}$ of phenylephrine, but it augmented the contractile response in aortic rings from arsenic-exposed animals. Sodium nitroprusside-induced relaxation was not altered with any treatment. However, arsenic reduced acetylcholine-induced relaxation and affected aortic eNOS at the levels of mRNA expression, protein concentration, phosphorylation and NO production. Further, it increased aortic iNOS mRNA expression, iNOS-derived NO synthesis, production of pro-inflammatory mediators (IL-1β, IL-6, MCP-1, VCAM, sICAM) and serum C-reactive protein and aortic vasculopathic lesions. Atorvastatin attenuated these arsenic-mediated functional, biochemical and structural alterations. Results show that atorvastatin has the potential to ameliorate arsenic-induced vascular dysfunction and inflammation by restoring endothelial function with improvement in NO signaling and attenuating production of pro-inflammatory mediators and cell adhesion molecules.



## Introduction

Arsenic as a contaminant in water and food chain or as inhaled particulates in the atmosphere is of great concern to human and animal wellbeing. However, contaminated groundwater is believed to be the major source of arsenic exposure. Human exposure takes place by direct intake of arsenic rich water (*via* drinking or cooked foods) or indirectly through food crops grown using arsenic-contaminated water. Arsenic contamination of groundwater and its impact on human health have been reported from several countries around the world. But the situation is worst in Asia, where groundwater contamination was reported in India, Bangladesh, Nepal, Vietnam, China, Taiwan and Japan (Jiang et al., 2013). A study revealed that one in five deaths in Bangladesh could be attributed to high arsenic exposure through drinking water and the WHO described this as the largest mass poisoning of a population in history (Argos et al., 2010). The magnitude of arsenic contamination is severe in Bangladesh followed by West Bengal, India. Serious health hazards can occur due to drinking of arsenic contaminated water for a period of about 5–15 years, but the duration can be even 2–5 years for high level exposure (Roy et al., 2013). Arsenic exposure was linked to increased risks of cancer and nonmalignant diseases, including cardiovascular diseases (CVDs) like hypertension, ischemic heart disease, atherosclerosis and peripheral vascular disease (Stea et al., 2014).

*Abbreviations:* ACh, acetylcholine; ATV, atorvastatin; CMC, carboxymethyl cellulose; CRP, C-reactive protein; CVD, cardiovascular disease; cNOS, constitutive nitric oxide synthase; ECs, endothelial cells; eNOS, endothelial nitric oxide synthase; ERK, extracellular signal regulated kinase; HMG CoA, 3-hydroxy-3-methylglutaryl-coenzyme A; IL-1β, interleukin-1 beta; IL-6, interleukin-6; iNOS, inducible nitric oxide synthase; LDL, low density lipoprotein; MCP-1, monocyte chemoattractant protein-1; MMAsIII, monomethyl arsenous acid; NO, nitric oxide; PE, L-phenylephrine; p-eNOS, phosphorylated-eNOS; sGC, soluble guanylyl cyclase; cGMP, cyclic nucleotide of guanosine monophosphate; sICAM, soluble intercellular adhesion molecule-1; SMCs, smooth muscle cells; SNP, sodium nitroprusside; TNF-α, tumor necrosis factor alpha; VCAM, vascular cell adhesion molecule; VED, vascular endothelial dysfunction.

* Corresponding author. Fax: +91 581 2303284.
*E-mail address:* snsarkar1911@rediffmail.com (S.N. Sarkar).

http://dx.doi.org/10.1016/j.taap.2014.07.008
0041-008X/

The endothelial cells (ECs) of blood vessels regulate vascular homeostasis by balancing production of vasodilators, including nitric oxide (NO) and vasoconstrictors. Vascular endothelial dysfunction (VED) is an early process in the event of various CVDs and it could result from impairment in NO activity (Virdis et al., 2010). Inflammation plays a pivotal role in VED. Arsenic produces or exacerbates inflammatory states and oxidative stress (States et al., 2009). Arsenic can enhance or reduce NO production, depending on the type of cell, species and dose (Gurr et al., 2003). Arsenite can suppress relaxation of rat blood vessels by inhibiting endothelial NO synthase (eNOS) activity (Lee et al., 2003). In humans, long-term exposure to arsenic-contaminated drinking water reduces NO production in the ECs partially due to inhibition of eNOS activity (Kumagai and Pi, 2004). Reduced bioavailability of endothelial NO is involved in the initiation and progression of atherosclerosis (Li and Forstermann, 2009). Deficiency of eNOS can accelerate atherosclerotic lesion formation in eNOS knockout mice (Kawashima and Yokoyama, 2004). Inducible NO synthase (iNOS) is induced in diseases associated with inflammation and oxidative stress (Sun et al., 2010). iNOS is up-regulated by arsenic and may contribute to the inflammatory response, increased reactive oxygen species generation, vascular remodeling, decreased aortic blood flow, attenuation of endothelium-dependent relaxation and endothelial cell damage (Sharma and Sharma, 2013; Steed et al., 2010).

Statins are the most effective and best-tolerated drugs for treating dyslipidemia and lowering cardiovascular risk associated with the elevation of low density lipoprotein (LDL) cholesterol. They are inhibitors of 3-hydroxy-3-methylglutaryl-coenzyme A (HMG-CoA) reductase, which catalyzes an early, rate limiting step in cholesterol biosynthesis (Bersot, 2011). They reduce the risk of both primary and secondary coronary heart disease, myocardial infarction, stroke and peripheral artery disease by lowering the LDL cholesterol and improving lipid profile. However, the clinical benefits of statin therapy may also be attributed to mechanisms independent of their cholesterol-lowering effects. The multiple cardioprotective effects of these drugs are ascribed to their pleiotropic effects, *viz*., anti-inflammatory, antioxidative, antiproliferative and immunosuppressive properties. Further, statins can increase NO bioavailability, neovascularization of ischemic tissue, circulation of endothelial progenitor cells and fibrinolysis, provide stability to atherosclerotic plaque, prevent platelet aggregation and thrombus formation and normalizes sympathetic outflow (Liao and Laufs, 2005). Efficacy of statins in reducing the risks of cerebrovascular diseases (Amarenco and Labreuche, 2009) and perivascular diseases (Aung et al., 2007) in humans was demonstrated.

Statins are prescribed for treating hyperlipidemia or atherosclerosis and once statin therapy is initiated, it is mostly continued for life. When a drug is being taken daily for a life-long period for treating hyperlipidemia and minimizing the risk of associated CVDs, if the same drug simultaneously possesses efficacy against arsenic-induced vascular dysfunction, it might provide an ameliorative measure for chronic arsenicosis. There is no proven treatment for chronic arsenic toxicity. Safe water, nutritious food, fruits, vegetables and physical exercise are the only preventive measures to combat arsenicosis. We wanted to understand whether statins could be a potential remedial measure for arsenic-induced VEDs. Biswas et al. (2010) demonstrated that atorvastatin (ATV) and N-acetyl cysteine treatment can synergistically recover the arsenic-induced death signaling in rat erythrocytes. Given that arsenic can induce and aggravate vascular disorders and statins have beneficial effects in CVDs, we assumed that statins could mitigate the risk of arsenic-induced development of VED, which eventually leads to development of CVDs in the arsenic-exposed subjects. Therefore, we evaluated whether ATV, an extensively prescribed statin, can reduce the risk of arsenic-induced vascular inflammation and dysfunction in rat model and whether the ATV-mediated modulation could be linked to improvement in vascular NO signaling.

## Materials and methods

*Drugs/kits/chemicals.* Sodium-*m*-arsenite (94%), acetylcholine (ACh), L-phenylephrine (PE) and sodium nitroprusside (SNP) were procured from Sigma-Aldrich, St. Louis, MO, USA. Atorvastatin (ATV) was purchased from Vivan Life Sciences, Mumbai (India). The EIA kits for assessing the levels of pro-inflammatory mediators, cell adhesion molecules, C-reactive protein (CRP) and eNOS were procured from Blue Gene Biotech, Inc., Shanghai, China. The Pathscan®136 #ser1177 phospho-eNOS sandwich ELISA kit was purchased from Cell Signaling Technology, Inc., USA. Chemicals for quantitative Real Time PCR *viz*., RNAlater®, Ribozol® were procured from Qiagen (Germany) and Amresco (USA), respectively, while Revertaid® Firststrand cDNA synthesis kit, Thermo Scientific Maxima SYBR Green/Fluorescein qPCR Master Mix (2X) from Thermo Fisher Scientific (USA). Carboxymethyl cellulose (CMC) sodium salt was purchased from G.S. Chemical Testing Lab and Allied Industries, Bombay. All other chemicals were of analytical or molecular grade.

*Dose/concentration selection.* The dose of ATV was selected from our earlier work, where effects of ATV on sepsis-induced VED were examined in rat thoracic aorta and pulmonary arteries (Subramani et al., 2009). There ATV at 10 mg/kg bw orally restored the impaired vascular endothelium-dependent relaxations mediated by NO and endothelium-derived hyperpolarizing factors. So we used ATV @ 10 mg/kg bw. Literature reveals that substantial progress in understanding the cardiovascular effects of arsenic has resulted from the studies conducted on specific genetic mouse models (*viz*., apolipoprotein E and low-density lipoprotein receptor double knockout or apolipoprotein E knockout mice) that make the mouse highly susceptible to the cardiovascular disorders (Simeonova et al., 2003; States et al., 2009). In these models, lower concentrations of arsenic through drinking water were shown to exacerbate vascular disorders. However, to simulate the natural arsenic exposure-mediated vascular disorders in a rat model – either normal rat (50 and 100 ppm of sodium arsenite; Sharma and Sharma, 2013; Yang et al., 2007) or even spontaneous hypertensive rat (100 ppm of arsenic; Cheng et al., 2011) – higher concentrations of arsenic were used. In a study on male Wistar rats, exposure to sodium arsenite at 50 ppm through drinking water for 200 successive days induced hypertension from the 80th day onwards, indicating development of vascular dysfunction (Yang et al., 2007). Since we exposed the male Wistar rats to arsenic for a subchronic duration of 90 days, we used 100 ppm of sodium arsenite to induce vascular dysfunction in order to examine the ameliorative effects of ATV. Further, this concentration is also relevant from an environmental perspective. The range of arsenic concentrations found in natural waters around the world vary from <0.0005 to >5 ppm (Rahaman et al., 2013). But there is a report that in West Bengal, India, people were exposed to arsenic-contaminated water in the range of 0.05–14.2 ppm (Guha Mazumder and Dasgupta, 2011). In the current study, the 100 ppm sodium arsenite used is equivalent to 57.7 ppm of elemental arsenic, which is about 4 times the 14.2 ppm environmental contamination level. Thus, considering the heterogeneity of drinking water resources and interspecies variation, the findings of the current study would be useful for risk assessment.

*Animals and experimental design.* The study was conducted on adult male Wistar rats (200–230 g) procured from the Laboratory Animals Resource Section of the Institute. They were housed in polypropylene cages with chopped wheat straw as the bedding material and given standard rat pellet feed (Amrut Feeds, Pranav Agro Industries Ltd, New Delhi, India) and provided water *ad libitum*. Before the commencement of the experiment, they were kept in laboratory conditions for 7 days for acclimatization. They were maintained under standard management conditions and handled as per the Institute Animal Ethics Guidelines.

Rats were divided randomly into 4 groups consisting of 12 each. Animals of Groups I and II received only drinking water, while those of Groups III and IV received 100 ppm of sodium arsenite through drinking water for 90 consecutive days. Further, the rats of Groups II and IV were administered ATV (10 mg/kg bw orally as aqueous suspension in 0.5% CMC) once daily during the last 30 days, *i.e.*, from day 61 to day 90. The remaining two groups received only vehicle (CMC) during the same period.

*Collection of blood and aorta.* On the 91$^{st}$ day, blood was collected from 6 rats/group by retro-orbital puncture under ketamine (80 mg/kg bw) and diazepam (2.2 mg/kg bw) anesthesia and taken into tubes (BD vacutainer®, 3.5 $cm^3$) coated with clot activator. The samples were centrifuged at 3500 rpm for 15 min and serum was stored at −80 °C till analysis of C-reactive protein.

After blood collection, the rats were killed by bleeding from posterior vena cava. Lungs and hearts from these animals were taken out *en block* along with the thoracic aorta and immediately placed in cold (4 °C) Modified Krebs Henseleit Solution [MKHS; composition (mmol/L): 118.0 NaCl, 4.7 KCl, 2.5 $CaCl_2.2H_2O$, 1.2 $MgSO_4$. 7 $H_2O$, 1.2 $KH_2PO_4$, 11.9 $NaHCO_3$ and 11.1 Glucose]. The thoracic aorta was isolated and the adhering tissues were removed. These aortas were used for *in vitro* (Organ Bath) assessment of their reactivity to vasoactive agents. Thoracic aortas from the remaining 6 animals of each group were trimmed, submerged in RNAlater® (Qiagen, Germany) at 4 °C overnight and stored at −20 °C until used for RNA extraction. Abdominal aortas from 6 animals of each group were collected, cleared of adhering tissue, snap frozen in liquid nitrogen and stored at −80 °C until ELISA of cytokines, chemokine and cell adhesion molecules. Thoracic aortas from additional 6 rats of another set of the same experimental design were isolated and used for measuring constitutive NOS (cNOS) and iNOS-mediated nitrite production.

*Tissue preparation and isometric recording.* The thoracic aortas were cut into 3–4 mm long rings. The aortic rings were mounted between two hooks made from 25 gauge stainless steel wire and kept under an optimal resting tension of 1.5 g in a thermostatically (37 ± 0.1 °C) controlled organ bath (UGO Basile, Comerio VA, Italy) of 10 ml capacity, containing MKHS and was continuously aerated with medical gas (74% $N_2$, 21% $0_2$ and 5% $CO_2$). The aortic rings were equilibrated for 60–80 min in the organ bath filled with MKHS before recording of tension. During equilibration period, the bath fluid was repeatedly changed once every 15 min. The change in tension was measured with a high-sensitivity isometric force transducer and recorded in a PC using Lab Chart 6 software program (Powerlab, AD Instruments, Australia).

After equilibration, arterial rings were contracted with high $K^+$ (80 mM)-depolarizing solution to check the viability of tissue. On attaining plateau, high $K^+$ solution was replaced with normal MKHS to restore the baseline resting tension. After 2–3 washes (within 50 min), contractions were elicited with cumulative addition of the $\alpha_1$-adrenoceptor agonist PE (1 nM–10 μM) to assess the response to a vasoconstrictor. Responses to vasodilators were assessed in PE-precontracted aortic rings. A submaximal concentration of PE (1 μM) was used to precontract the tissue and cumulative concentration-dependent relaxation to endothelium-dependent vasodilator ACh (1 nM–10 μM) and the endothelium-independent nitro-vasodilator SNP (0.1 nM–10 μM) were produced.

*Quantitative Real-Time PCR analysis of eNOS and iNOS genes.* The thoracic aorta collected in RNAlater solution was taken out and about 75 mg of tissue was homogenized in microcentrifuge tube containing 1 ml Ribozol™ reagent (Amresco LLC., OH, USA) with Polytron homogenizer. Chloroform (200 μl) was mixed with the homogenate. The mixture was vortexed for 30 s, kept for 10 min at room temperature and centrifuged at 12,000 ×*g* for 15 min to separate the homogenate into 3 layers. The top aqueous layer was collected, from which the RNA was precipitated with equal volume of ice-cold isopropanol. It was mixed properly and kept for 10 min at room temperature. Then centrifugation was done at 12,000 ×*g* for 10 min at 4 °C. The supernatant was discarded and RNA pellet was collected. RNA pellet was washed with 75% ethanol at 7500 ×*g* for 5 min. The pellet was air dried and ≈40 μl nuclease-free water was added to the pellet. The purity of the RNA was quantified by NanoDrop® spectrophotometer and only RNA samples with an A260/A280 ratio of 1.8–2.0 were used for reverse transcription.

cDNA synthesis was carried out using Revertaid® First strand cDNA synthesis kit from Thermo Fisher Scientific, USA. cDNA was synthesized from the mRNA present in the total RNA using moloney murine leukemia virus (MMLV) reverse transcriptase. The respective primers used for expression of the eNOS (Gragasin et al., 2004), iNOS (Scumpia et al., 2002) and β-actin (Wang et al., 2005) genes were F 5′-TTACTTCCTGGACATCACTTCCC-3′, R 5′-AGCACCCTGGCAGAGG AGT-3′ (70 bp); F 5′-AGCGGCTCCATGACTCTC-3′, R 5′-CGGACCATCT CCTGCATT-3′ (118 bp) and F 5′-AGTGTGACGTTGACATCCGT-3′, R 5′-GACTCATCGTACTCCTGCTT-3′ (244 bp).

qRT-PCR reactions were run on Real-Time PCR (Bio Rad T100™ thermal Cycler) and analyzed using Bio Rad CFX Manager Software. Real-Time PCR was conducted using SYBR Green I master mix [Thermo Scientific Maxima SYBR Green/Fluorescein qPCR Master Mix (2X) (Thermo Fisher Scientific, USA)]. The optimum annealing temperatures as determined by PCR for β-actin, eNOS and iNOS using the specific primers were 60 °C, 58 °C, and 52 °C, respectively. Each sample was run in duplicate in 25 μl reaction. The 25 μl reaction mixture contained 12.5 μl SYBR Green master mix, 0.5 μl from 10 pmol working solution of each of gene specific forward and reverse primers, 1 μl of cDNA and the volume was made up to 25 μl with Nuclease-free water. The real time PCR reaction was started with initial incubation at 95 °C for 15 min followed by 40 cycles of amplification with denaturation at 95 °C for 30 s, annealing at 60 °C for 30 s and extension at 72 °C for 30 s for each cycle. To assess the specificity of the amplified product, dissociation curve was generated at temperature 60 °C through 95 °C. The result was expressed as threshold cycle ($C_T$).

To study the relative change in gene expression the $2^{-\Delta\Delta CT}$ method was used as described previously (Livak and Schmittgen, 2001). The formula used to calculate the fold change in gene expression was, fold change $= 2^{-\Delta\Delta CT}$, where $\Delta\Delta C_T$ = ($C_T$ of target gene − $C_T$ of β-actin) treatment − ($C_T$ of target gene − $C_T$ of β-actin) control. The gene specific amplification was corrected for the difference in input of RNA by taking housekeeping gene β-actin into account. The results were analyzed in comparison to the $C_T$ value of the target gene and the reference gene.

*Preparation of aortic homogenate.* The abdominal aorta was cut into small pieces and taken in microcentrifuge tubes. For 100 mg tissue, 1 ml of PBS (pH 7.4) with mammalian protease inhibitor cocktail [4-(2-Aminoethyl) benzenesulfonyl fluoride, 1.20 mM; Aprotinin, 0.46 μM; Bestatin, 14 μM; E-64, 12.30 μM; Leupeptin, 112 μM and Pepstatin, 1.16 μM (Amresco LLC., OH, USA)] was added and homogenized with polytron homogenizer. The homogenate was centrifuged at 1800 ×*g* for 15 min at 4 °C and the supernatants were stored at 4 °C for immediate analysis.

*ELISA of aortic eNOS protein, cytokines, chemokine, cell adhesion molecules and serum acute phase protein.* Estimations of pro-inflammatory cytokines, *viz.*, interleukins (IL-1β and IL-6), chemokine, *viz.*, monocyte chemoattractant protein-1 (MCP-1), cell adhesion molecules such as vascular cell adhesion molecule-1 (VCAM-1) and soluble intercellular adhesion molecule-1 (sICAM-1) and eNOS protein in the aortic homogenate and C-reactive protein (CRP), an acute phase protein, in serum were carried out with the EIA kits as per the manufacturer's instructions (Blue Gene Biotech, Inc. Shangai, China).

*Estimation of phosphorylated-eNOS.* The phosphorylated form of eNOS (p-eNOS), *i.e.* the functional eNOS was assessed by ELISA in the aortic homogenate using Pathscan®#ser1177 phospho eNOS sandwich ELISA kit (Cell Signaling Technology, Inc., USA) as per the manufacturer's protocol.

*Assessment of NO production.* Formation of NO was measured as nitrite as described previously by Zhang et al. (1999). Briefly, endothelium-intact rat thoracic aortas of treatment groups were collected in ice-cold MKHS and adherent fat tissue and debris were removed. The aortas were cut into small rings and placed in a 2 ml plastic tube that contained 500 μL of MKHS as control or 5 μL of 1400 W (1 mM; final concentration 10 μM), a selective iNOS inhibitor, and the final volume was adjusted to 500 μL with MKHS. All the tissues were incubated for 60 min at 37 °C with continuous aeration in water bath. After incubation, the aortic rings were removed and 450 μL of sulfanilamide (1%) and 50 μL of N-(1-naphthyl) ethylenediamine (0.2%) were added to each tube for diazotization of sulfanilic acid by NO. After 20 min of incubation at 37 °C, absorbance was measured by a spectrophotometer at 540 nm and compared with the known concentration of nitrite. To construct the standard curve, the same procedure was followed except that individual tubes contained 1, 2.5, 5, 7.5 or 10 μM of nitrite diluted from a stock solution of $NaNO_2$ (10 mM). Absorbance was measured and converted to a straight line with regression analysis ($Y = ax + b$, $R > 0.99$). Values of nitrite were derived from the linear regression formula. Data were expressed as mean ± S.E. in pmol/mg wet tissue. cNOS-derived NO was measured as the nitrite produced in the presence of 1400 W, while total nitrite level minus cNOS-derived nitrite production was taken as iNOS-derived nitrite or NO production.

*Histopathology.* Aortic arches from all the groups were fixed in 10% neutral buffered-formalin. The tissues were dehydrated in ascended alcohol series and embedded in paraffin wax. Approximately 5-μm thick sections were cut, deparaffinized by dipping in xylene for 15 min and stained with hematoxylin and eosin for the assessment of histological alterations under light microscopy (Leica Microsystem, Germany). Histological scoring was done using Leica Qwin image analysis software.

*Statistical analysis.* Aortic relaxation responses have been expressed as the percentage reversal of the PE contraction. Both $E_{max}$ and $EC_{50}$ were determined by nonlinear regression analysis using GraphPad Prism version 4.00 (San Diego, California, USA). Potency has been expressed as $PD_2 = -\log EC_{50}$. Data have been expressed as mean ± S.E. with 'n' equal to number of vascular rings or number of animals. Data of organ bath studies were analyzed by two way ANOVA followed by Bonferroni *post hoc*-test. All other data were analyzed by one way ANOVA followed by Newman Keuls *post hoc* test. Difference at $p < 0.05$ was considered statistically significant.

## Results

*Effects of ATV on ACh-induced endothelium-dependent relaxation in the arsenic-exposed aorta*

Aortic rings from the control animals showed dose-dependent relaxation to ACh and the $pD_2$ and $E_{max}$ were 7.58 ± 0.01 and 102.7 ± 1.84%, respectively (Fig. 1A). ATV produced similar dose response to ACh ($pD_2$: 7.64 ± 0.17 and $E_{max}$: 96.2 ± 1.22%). As shown in Fig. 1A, arsenic exposure significantly decreased the efficacy (80.34 ± 2.176%) of ACh but not the potency (7.54 ± 0.04). ATV treatment in arsenic-exposed animals, significantly improved the efficacy (101.7 ± 4.12%) but not the potency (7.47 ± 0.09).

*Effects of ATV on SNP-induced relaxation in the arsenic-exposed aorta*

Fig. 1B depicts the effects of ATV on SNP-induced relaxation in rat aorta. The aortic relaxation with SNP was not altered with arsenic, ATV or with their concurrent exposure. The respective $pD_2$ values of the control, ATV, arsenic and arsenic/ATV groups were 8.23 ± 0.04, 8.45 ± 0.07, 8.18 ± 0.16 and 8.35 ± 0.11, while the $E_{max}$ values were 107.5 ± 1.30, 102.2 ± 1.67, 112.6 ± 4.53 and 101 ± 2.49%.

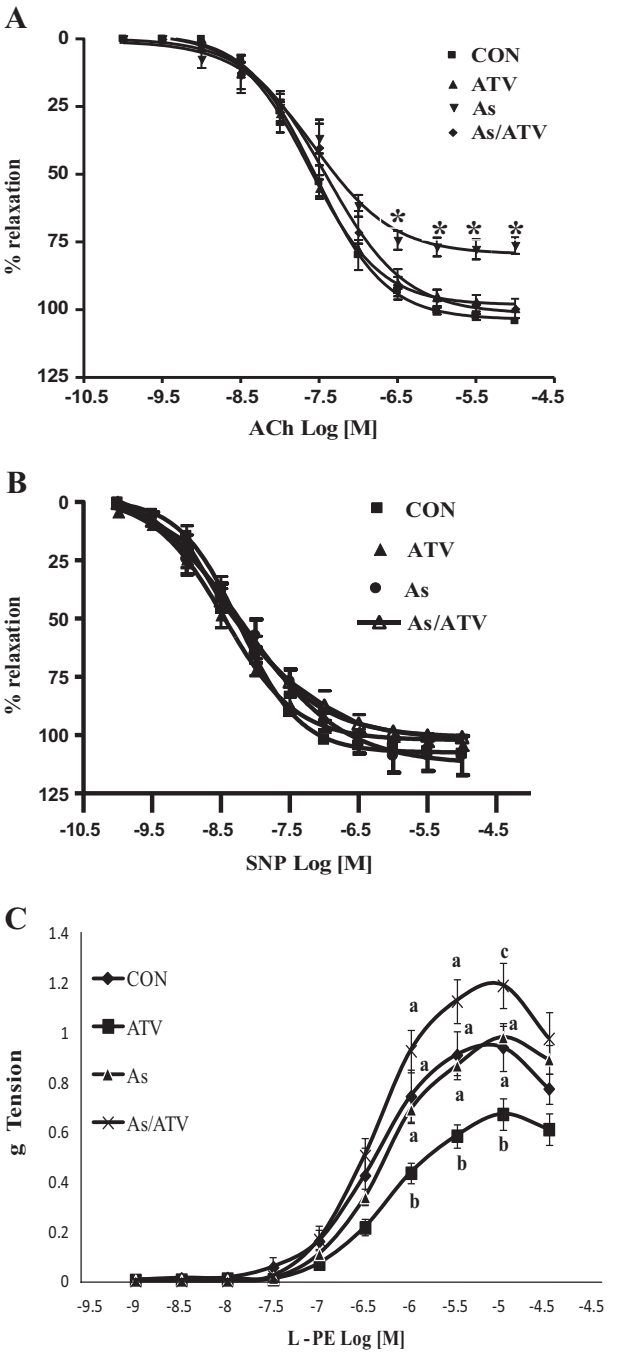


**Fig. 1.** Effects of atorvastatin on acetylcholine (ACh) [A] and sodium nitroprusside (SNP) [B]-induced relaxation and phenylephrine (PE)-elicited contraction [C] in the arsenic (As)-exposed rat aorta. Values are mean of 6 rats and vertical bars represent standard errors. *$p < 0.05$ in comparison to control (CON), atorvastatin (ATV) and arsenic/atorvastatin (As/ATV) in Bonferroni test. In the case of PE concentration-response, values of the same concentration point bearing different superscripts vary significantly ($p < 0.05$) in Bonferroni test.

*Effects of ATV on PE-induced contractile response in the arsenic-exposed aorta*

Fig. 1C illustrates the effects of ATV on PE-induced contraction (g tension) in rat aorta. The aortic rings from the control animals exhibited concentration-dependent contractions to PE. The control $pD_2$ and $E_{max}$ values were 6.49 ± 0.09 and 0.88 ± 0.05 g, respectively. ATV significantly reduced the efficacy of PE to 0.65 ± 0.03 g but did not alter the potency (6.25 ± 0.07 g). Arsenic did not alter the PE-induced contractions ($pD_2$: 6.32 ± 0.04; $E_{max}$: 0.94 ± 0.02 g). However, ATV treatment significantly augmented the dose response ($pD_2$: 6.46 ± 0.06; $E_{max}$: 1.11 ± 0.04 g).

*Effects of ATV on eNOS mRNA expression in the arsenic-exposed aorta*

The eNOS mRNA expression (fold change) is depicted in Fig. 2A. The expression of eNOS mRNA in the ATV-treated group (2.07 ± 0.43) was not significantly different from that in the control rats (1 ± 0.0). Subchronic exposure to arsenic caused its significant down-regulation (0.24 ± 0.12). ATV significantly reversed (1.44 ± 0.24) the effect of arsenic on eNOS expression.

*Effects of ATV on total eNOS protein level in the arsenic-exposed aorta*

Fig. 2B shows the effects on the total eNOS protein level (pg/mg of wet tissue) in aortic tissue. In the control animals, the level was 59.21 ± 3.33. ATV did not alter its level significantly 55.68 ± 2.03. Arsenic significantly reduced the concentration of eNOS (45.1 ± 1.73). In the arsenic-exposed rats, ATV significantly increased (58.28 ± 3.65) it to the control level.

*Effects of ATV on phosphorylated eNOS concentration in the arsenic-exposed aorta*

Effects on the levels of p-eNOS (OD value) are summarized in Fig. 2C. The OD value of the ATV-treated group (0.77 ± 0.11) was statistically similar to that of the control value (0.74 ± 0.09). Arsenic alone significantly reduced its value to 0.38 ± 0.02, which was significantly attenuated (0.61 ± 0.03) with ATV in the arsenic-exposed rats.

*Effects of ATV on cNOS-mediated nitrite production in the arsenic-exposed aorta*

Effects on the levels of cNOS-mediated nitrite production (pmol/mg wet tissue) have been presented in Fig. 2D. In the control rats, its level was 37.52 ± 1.88. ATV significantly increased it to 48.82 ± 2.96. But arsenic exposure significantly decreased the nitrite level to 29.91 ± 1.21. However, in the arsenic exposed rats, ATV significantly increased its level to 54.07 ± 2.78.

*Effects of ATV on iNOS mRNA expression and iNOS-mediated nitrite production in the arsenic-exposed aorta*

The mRNA expression (fold change) of iNOS gene is presented in Fig. 3A. Compared to that in the control rats (1.00 ± 0.0), ATV significantly down-regulated (0.214 ± 0.132) its expression, while arsenic caused its significant up-regulation to 1.67 ±0.37. However, ATV caused significant reversal of the arsenic-mediated up-regulation of iNOS expression to 0.318 ± 0.17.

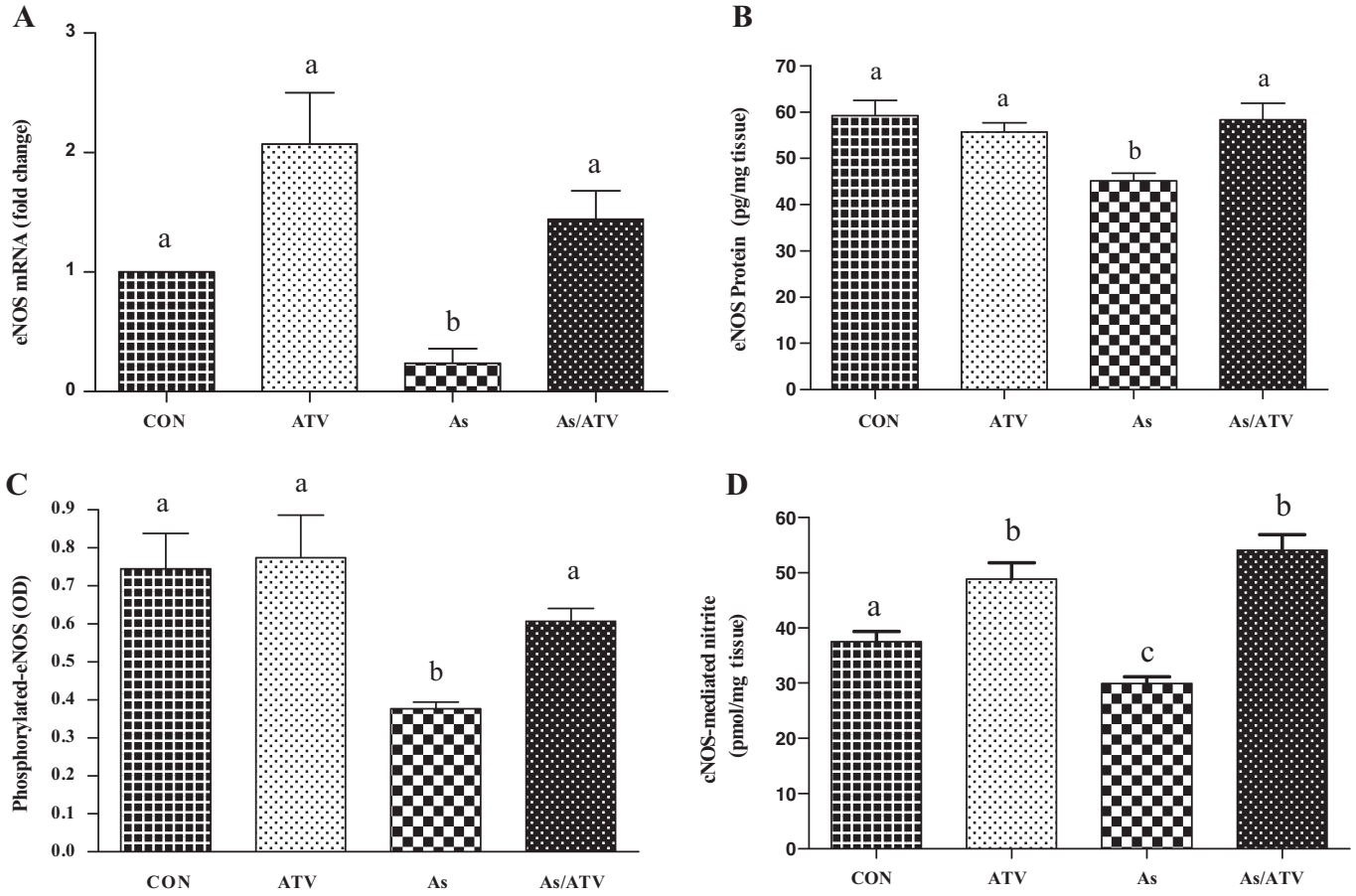


**Fig. 2.** Effects of atorvastatin on endothelial nitric oxide synthase (eNOS) gene expression [A], eNOS protein level [B], phosphorylated (P-eNOS) protein concentration [C] and constitutive nitric oxide synthase (cNOS)-induced nitrite production [D] in the arsenic-exposed rat aorta. CON: control; ATV: atorvastatin; As: arsenic; As/ATV: arsenic/atorvastatin. Bars (mean ± SE; n = 6) bearing different superscripts vary significantly ($p < 0.05$) in Newman–Keuls test.

Fig. 3B shows the effects on the levels of iNOS-mediated nitrite production (pmol/mg wet tissue). Control level of nitrite production was 14.18 ± 1.83. ATV significantly decreased its level to 4.74 ± 1.23. But arsenic exposure significantly increased the level to 73.11 ± 4.46. However, ATV brought the nitrite production back to the level (8.42 ± 0.83), which was comparable to the control value.

*Effects of ATV on pro-inflammatory cytokines, chemokine, cell adhesion molecules and acute phase protein levels in the arsenic-exposed aorta*

Effects on the levels of pro-inflammatory cytokines, *i.e.*, IL-1β and IL-6 (pg/mg wet tissue) are summarized in Table 1. The respective levels of IL-1β and IL-6 in the control rats were 3.30 ± 0.26 and 31.43 ± 4.38. ATV did not alter these levels (2.84 ± 0.27 and 25.37 ± 2.81) appreciably. Arsenic exposure significantly increased their levels to 5.80 ± 0.48 and 50.55 ± 5.99. ATV significantly attenuated the arsenic-mediated increase statistically to their respective control levels (3.37 ± 0.20 and 26.47 ± 2.23).

Table 1 presents the effects on MCP-1 level (pg/mg wet tissue). In the control group, its level was 21.17 ± 3.36 and it was not altered with ATV (17.07 ± 1.13). Arsenic significantly increased its level to 39.56 ± 4.52. However, in the arsenic-exposed animals, ATV significantly reduced the level to 15.45 ± 1.81, which was comparable to the control value.

The aortic concentrations of the cell adhesion molecules such as VCAM-1 and sICAM-1 (pg/mg wet tissue) are shown in Table 1. The respective concentrations of these adhesion molecules were 209.9 ± 15.84 and 262.9 ± 11.07 in the control rats. ATV did not significantly alter their levels (171.2 ± 6.74 and 279.8 ± 9.61). Exposure of the rats to arsenic significantly increased the VCAM-1 level to 345.5 ± 31.61 and the sICAM-1 level to 359.5 ± 21.93. ATV significantly reduced the arsenic-mediated increase in their concentrations and brought their levels statistically back to the respective control level (186.5 ± 14.27 and 280.8 ± 11.14).

The levels of serum CRP, an acute phase protein, concentration (μg/ml serum) are presented in Table 1. ATV did not cause any significant alteration (1.47 ± 0.26) in its level compared to the control level (1.52 ± 0.17). Arsenic significantly increased its level to 2.83 ± 0.34. However, ATV significantly reduced (1.88 ± 0.26) its level in the arsenic-exposed animals comparably to the control level.

*Histological evaluation*

Table 2 and Figs. 4A, B show that the control and the ATV-treated rats did not show any appreciable alterations in the aortic arch. Arsenic exposure caused increase in the number of mononuclear cell infiltration and higher incidences of fatty streaks, foam cell formation, focal intimal thickening and disrupted smooth muscle integrity (Table 2; Figs. 4C–E). ATV appreciably attenuated these vascular histological lesions in the arsenic-exposed rats (Table 2; Fig. 4F).

## Discussion

Several reports reveal that arsenic causes vascular dysfunctions, alterations in vascular histology (Cheng et al., 2011; Lee et al., 2003; Sharma and Sharma, 2013; Verma et al., 2010) and hypertension (Yang et al., 2007) in Wistar or Sprague-Dawley rats. Accordingly, we chose rat as the model for assessing arsenic-induced vascular dysfunction and took the aorta as the model vascular tissue. The objective of the current study was to evaluate whether atorvastatin can reduce the arsenic-induced vascular dysfunction and inflammation. The major findings of the study: arsenic reduced ACh-induced relaxation, interfered with NO signaling by inhibiting eNOS and inducing iNOS, enhanced production of pro-inflammatory mediators and produced histological lesions in the aorta. ATV attenuated these arsenic-mediated functional, biochemical and structural alterations, showing its potential to ameliorate arsenic-induced vascular dysfunction in rats.

Arsenic did not alter SNP-induced relaxation, indicating that the soluble guanylyl cyclase (sGC) pathway was not affected. There are reports showing that arsenic did not alter SNP-induced relaxation of aortic rings (Verma et al., 2010; Sharma and Sharma, 2013) in Wistar rats. The PE dose–response was also not altered by arsenic. ATV inhibited PE-elicited contraction ($E_{max}$), which is consistent with the observation made in mouse aorta (Kandasamy et al., 2011). However, it augmented the contractile response in the arsenic-exposed animals. This finding needs further studies to elucidate the $\alpha_1$-adrenoceptor modulation in the arsenic/ATV-treated rats.

Vascular ECs are considered the primary target of vasculopathy induced by arsenic (Tsou et al., 2005). Impairment of endothelium-dependent vasorelaxation because of reduced NO bioavailability due to decreased eNOS activity is a VED that results in deregulation of vascular homeostasis and increased adhesiveness of the endothelium lining for circulating inflammatory cells (Rang et al., 2012). Arsenic-mediated reduction in the aortic relaxation to ACh and our findings on the markers of vascular inflammation and histology are the obvious evidences of VED. The arsenic-mediated inhibition of aortic relaxation to ACh is in agreement with the findings of other workers (Verma et al., 2010; Sharma and Sharma, 2013) and this may relate to altered NO signaling.

Arsenic downregulated eNOS and upregulated iNOS expression. A similar effect was observed in the kidney following exposure of Wistar rats to arsenic at 25-ppm *via* drinking water for 59 days (Majhi et al., 2011). Prabu and Muthumani (2012) also reported renal iNOS up-regulation with arsenic in Wistar rats. Besides eNOS protein level, eNOS phosphorylation is thought to regulate enzyme activity in both

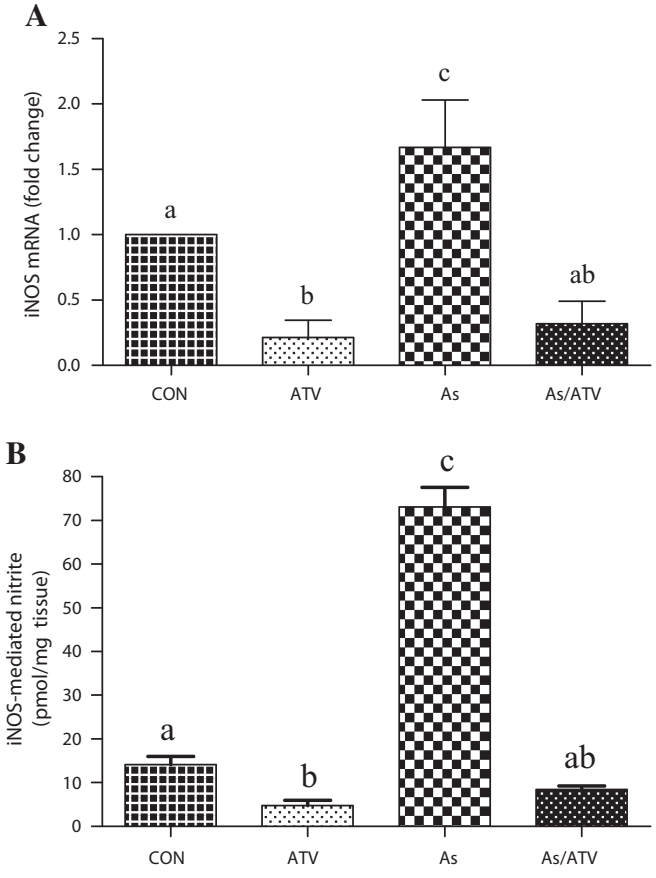


**Fig. 3.** Effects of atorvastatin on inducible nitric oxide synthase (iNOS) mRNA expression [A] and iNOS-mediated nitrite production in the arsenic-exposed rat aorta. CON: control; ATV: atorvastatin; As: arsenic; As/ATV: arsenic/atorvastatin. Bars (mean ± SE; n = 6) bearing no superscripts common vary significantly ($p < 0.05$) in Newman–Keuls test.

**Table 1**
Effects of atorvastatin on the levels of aortic cytokines, chemokine and cell adhesion molecules and serum acute phase protein in the arsenic-exposed rats.

| Treatment | Cytokine | | Chemokine | Cell adhesion molecule | | Acute phase protein |
|---|---|---|---|---|---|---|
| | IL-1β (pg/mg tissue) | IL-6 (pg/mg tissue) | MCP-1 (pg/mg tissue) | VCAM-1 (pg/mg tissue) | sICAM-1 (pg/mg tissue) | CRP (μg/ml serum) |
| Control | 3.30 ± 0.26[a] | 31.43 ± 4.38[a] | 21.17 ± 3.36[a] | 209.9 ± 15.84[a] | 262.90 ± 11.07[a] | 1.52 ± 0.17[a] |
| Atorvastatin | 2.84 ± 0.27[a] | 25.37 ± 2.81[a] | 17.07 ± 1.13[a] | 171.2 ± 6.74[a] | 279.80 ± 9.61[a] | 1.47 ± 0.26[a] |
| Arsenic | 5.80 ± 0.48[b] | 50.55 ± 5.99[b] | 39.56 ± 4.52[b] | 345.5 ± 31.61[b] | 359.50 ± 21.93[b] | 2.83 ± 0.34[b] |
| Arsenic/atorvastatin | 3.37 ± 0.20[a] | 26.47 ± 2.23[a] | 15.45 ± 1.81[a] | 186.5 ± 14.27[a] | 280.80 ± 11.14[a] | 1.88 ± 0.26[a] |

Arsenic exposure was given as sodium arsenite at 100 ppm through drinking water for 90 days. Atorvastatin (10 mg/kg bw) was administered by oral gavage as aqueous suspension in 0.5% carboxymethyl cellulose once daily during the last 30 days of arsenic exposure. Values (mean ± SE; n = 6) in the same column bearing different superscripts vary significantly ($p < 0.05$) in Newman–Keuls test. IL-1β: interleukin-1β; IL-6: interleukin-6; MCP-1: monocyte chemoattractant protein-1; VCAM-1: vascular cell adhesion molecule-1; sICAM-1: soluble intercellular adhesion molecule-1; CRP: C-reactive protein.

$Ca^{2+}$-calmodulin-dependent and $Ca^{2+}$-calmodulin-independent fashion (Dimmeler et al., 1999; Fulton et al., 2001). To know whether eNOS gene expression is translated into protein, we measured the level of aortic eNOS protein content. Furthermore, to evaluate the functional eNOS, we assessed the level of p-eNOS. Arsenic reduced both the eNOS protein and the p-eNOS. These indicate that arsenic affected the eNOS at transcriptional, translational and post-translational levels. Impairment of eNOS function by arsenite is believed one of the mechanisms leading to vascular changes and diseases (Tsou et al., 2005). Sodium arsenite caused VED decreasing ACh-induced vasorelaxation (Jindal et al., 2008) by increasing the oxidative stress and reducing eNOS concentration (Kaur et al., 2010). Monomethyl arsenous acid (MMAsIII), which is the most toxic metabolic intermediate of sodium arsenite in rats and humans (Styblo et al., 2000) and believed to be the cause of chronic arsenic toxicity (Csanaky et al., 2003), inhibited eNOS activity (Sumi, 2008). Further, several studies suggest that arsenic causes down-regulation of vascular eNOS, resulting in decreased NO production (Lee et al., 2003; Pi et al., 2003; Tsou et al., 2005).

An increase in the basal NO production at the picomolar range, as in case of eNOS, tends to restore endothelial function, whereas large increase in the NO production in the nanomolar range, as is typical of iNOS activity, may promote cell damage. Therefore, an increase in eNOS by statins accompanied by a simultaneous reduction in iNOS activity could give endothelial protective effects (Wayman et al., 2003). ATV increased eNOS and decreased iNOS expression in aorta of septic rats (Subramani et al., 2009) and in mesenteric artery of ovariectomized rats (Caliman et al., 2013). Further, ATV inhibited cytokine-stimulated iNOS expression in the ECs of rat aorta (Wagner et al., 2002). It is known that eNOS is the major contributor of vascular cNOS-mediated NO production. Hence, to understand the contribution of NOS isozyme-derived NO, we measured cNOS and iNOS-derived nitrite production in aorta. In our model, ATV increased cNOS-derived NO production with no alteration in basal eNOS protein, p-eNOS or its mRNA expression. But it caused down-regulation of iNOS gene and reduction in iNOS-derived NO synthesis. On the other hand, arsenic downregulated eNOS and decreased cNOS-mediated NO level, while it upregulated iNOS gene and increased iNOS-derived nitrite production. In the arsenic-exposed rats, ATV restored the levels of nitrite production by these isozymes. This indicates that the restoration of ACh-induced relaxation in the arsenic-exposed aorta could be due to normalization of the effects of arsenic on NO production. Thus, attenuation of arsenic-stimulated down-regulation of eNOS and up-regulation of iNOS could be a mechanism by which ATV may normalize NO signaling in aorta and attenuate the development of aortic dysfunction in the arsenic-exposed rats.

VED in terms of vasomotor dysfunction can occur well before the structural manifestation and inflammatory process of atherosclerosis and thus can serve as an independent predictor of cardiovascular events. NO is a buffer against pro-inflammatory mechanisms (Chen et al., 2001). Studies reveal that NO inhibits leukocyte adhesion to endothelium, maintains vascular smooth muscle cells (SMCs) in a nonproliferative state and limits platelet aggregation (Szmitko et al., 2003). eNOS is the primary isoform responsible for the production of NO within blood vessels (Huang et al., 1995) and the loss of eNOS increases the development of chronic inflammatory disorders. NO suppresses endothelial ICAM-1 expression *via* a sGC/cGMP-independent signaling process (Niu et al., 1994). One proposed mechanism is through the inhibition of NF-κB (Matthews et al., 1996), which is activated in response to cytokines and promotes increased transcription of genes, including ICAM-1 and VCAM-1, having κB sites in their promoters (Janssen-Heininger et al., 2000). Our results show that the availability of eNOS-derived NO was less in the arsenic-exposed rats and this could be an underlying reason for enhanced aortic inflammation.

Tissue and plasma concentrations of the markers of vascular inflammation and VED are increased in patients with CVDs (Blake and Ridker, 2001). Those markers include CRP, adhesion molecules (VCAM-1, ICAM-1) and chemokines (MCP-1). In response to injury or inflammatory stimuli, ECs express VCAM-1, ICAM-1 and selectins on the cell surface (Kasper et al., 1996). The selectins mediate transient rolling of the leukocytes along the endothelium (Tedder et al., 1995), while stronger attachment is mediated by ICAM-1 and VCAM-1 (Springer, 1994). Expression of cell adhesion molecules is induced by pro-inflammatory cytokines (*e.g.*, IL-1β and TNF-α) and CRP that is produced by the liver in response to IL-6 and TNF-α (Szmitko et al., 2003) as part of the non-specific acute-phase response to tissue damage, infection, inflammation and malignant neoplasia (Savoia and Schiffrin, 2006).

**Table 2**
Effects of atorvastatin on the histopathological alterations in the arsenic-exposed rats.

| Animal number | Control | | | | | Atorvastatin | | | | | Arsenic | | | | | Arsenic/atorvastatin | | | | |
|---|---|---|---|---|---|---|---|---|---|---|---|---|---|---|---|---|---|---|---|---|
| | FT | FC | FS | MNC | SMI* | FT | FC | FS | MNC | SMI* | FT | FC | FS | MNC | SMI* | FT | FC | FS | MNC | SMI* |
| 1 | 0 | 0 | 0 | 0 | ++++ | 0 | 0 | 0 | 0 | ++++ | 2 | 9 | 2 | 13 | + | 0 | 2 | 1 | 2 | +++ |
| 2 | 0 | 0 | 0 | 0 | ++++ | 0 | 0 | 0 | 0 | ++++ | 2 | 7 | 1 | 15 | + | 0 | 0 | 0 | 3 | ++++ |
| 3 | 0 | 0 | 0 | 0 | ++++ | 0 | 0 | 0 | 0 | ++++ | 1 | 5 | 0 | 9 | ++ | 0 | 1 | 0 | 0 | +++ |
| 4 | 0 | 0 | 0 | 0 | ++++ | 0 | 0 | 0 | 0 | ++++ | 1 | 6 | 1 | 11 | + | 1 | 2 | 1 | 1 | ++ |
| 5 | 0 | 0 | 0 | 1 | ++++ | 0 | 0 | 0 | 0 | ++++ | 2 | 10 | 3 | 13 | ++ | 0 | 0 | 0 | 0 | +++ |
| 6 | 0 | 0 | 0 | 0 | ++++ | 0 | 0 | 0 | 0 | ++++ | 3 | 13 | 2 | 6 | + | 0 | 0 | 0 | 2 | ++ |
| Total | 0 | 0 | 0 | 1 | – | 0 | 0 | 0 | 0 | – | 11 | 50 | 9 | 67 | – | 2 | 10 | 4 | 16 | – |

Numerical values under each treatment group indicate number of lesions observed per 10 fields/section/animal (H&E × 400). FT: focal thickening; FC: foam cell; FS: fatty streak; MNC: mononuclear cells, *SMI: smooth muscle integrity. Scoring of SMI was done in 10 fields/section/animal in the scale of + to ++++, where ++++ indicates normal smooth muscle integrity.

CRP contributes to arterial inflammation by directly increasing the release of endothelin-1 and up-regulating cell adhesion molecules and chemoattractant chemokines in ECs, monocytic cells and vascular SMCs (Paffen and deMaat, 2006). Thereby, CRP can activate the entire recruitment cascade (Yeh, 2004) and monocyte diapedesis (Paffen and deMaat, 2006). The monocyte migration is directed along a concentration gradient of MCP-1 *via* interaction with the monocyte receptor (Szmitko et al., 2003). The chemotactic cytokine MCP-1 is produced by ECs after exposure to cytokines (IL-1β, IL-6, TNF-α), CRP (Rott et al., 2003) and oxidized lipoproteins (Papayianni et al., 2002). MCP-1 plays an important role in the migration and activation of monocytes and T cells and moreover, regulates the proliferation of vascular SMCs (Papayianni et al., 2002). In the intima, lipoprotein particles (LDL and oxidized LDL) that accumulate in the lesion are taken up by monocyte-derived macrophages, leading to formation of lipid-laden macrophages (foam cells) and fatty streak. The cells involved in foam cell formation (*e.g.* ECs, monocytes, T-cells, SMCs) begin to secrete different substances, including cytokines (IL-6, TNF-α, IL-1), chemokines (MCP-1, interleukin-8) and CRP (Paffen and deMaat, 2006), which maintain a chemotactic stimulus for adherent leukocytes, augment expression of scavenger receptors and promote macrophage replication.

Our findings show that arsenic increased the levels of inflammatory cytokines (IL-1β, IL-6), the chemokine (MCP-1), acute phase protein (CRP) and cell adhesion molecules (VCAM-1, sICAM-1) and also produced aortic lesions, providing evidence for aortic inflammation

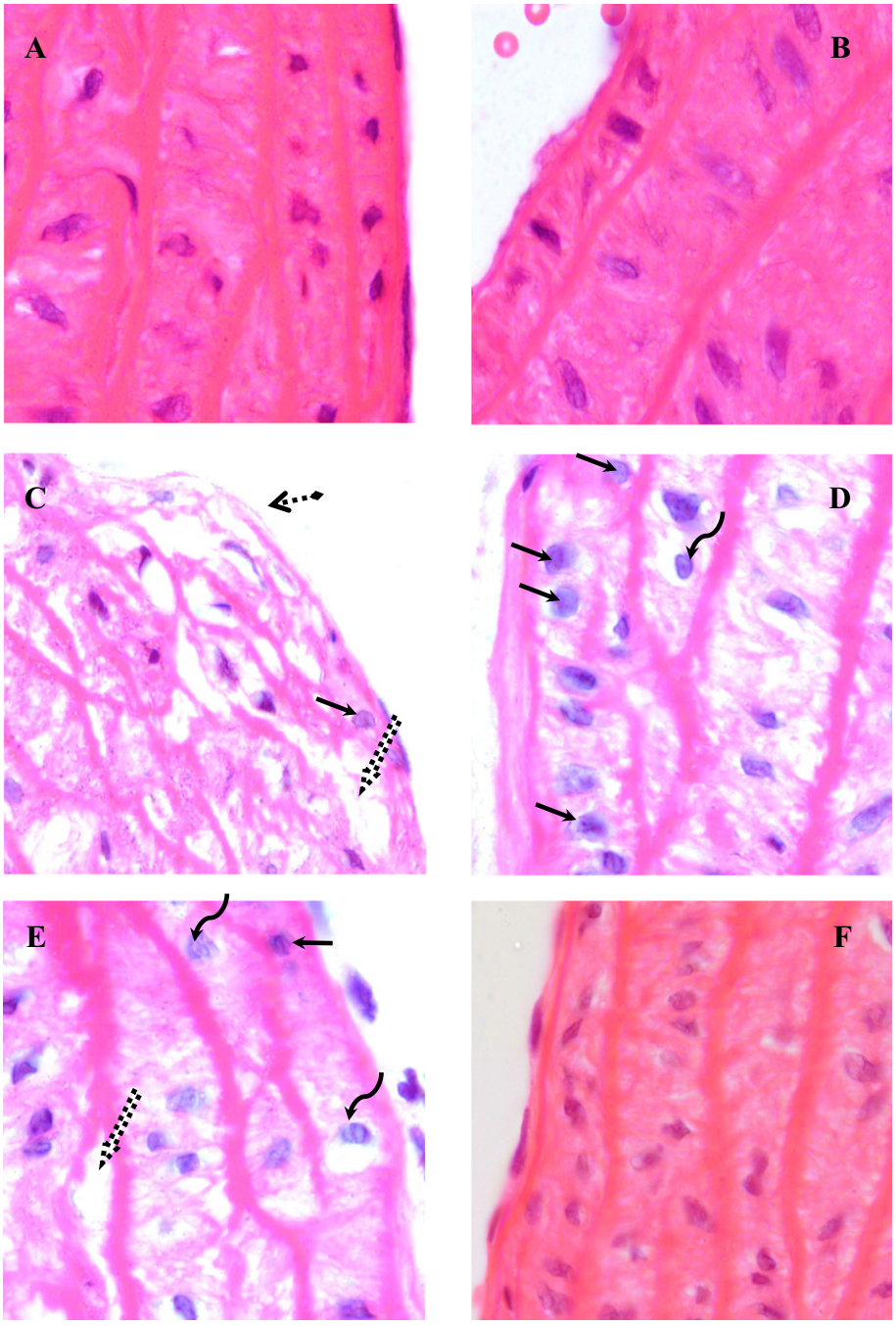


**Fig. 4.** Photomicrographs showing normal histology of aortic arch in the control (A) and atorvastatin (B)-treated rats. Photomicrographs of the arsenic-exposed aortic arch (C, D, E) showing fatty streaks (⁘), focal thickening (⇢), foam cell (↘), mononuclear cell infiltration (⟶) and impairment of smooth muscle integrity. Photomicrographs of aortic arch of the arsenic/atorvastatin-treated group (F) showing histological features comparable to those of the control rats. H&E × 1000.

and dysfunction. Studies showed that exposure to arsenic enhanced vascular inflammation and plasma concentrations of MCP-1, IL-6, VCAM-1, sICAM-1 (Chen et al., 2007; Srivastava et al., 2009) and CRP (Cheng et al., 2011). Further, the vasculopathic lesions in the aorta, *i.e.*, increased mononuclear cell infiltration, fatty streak, foam cell, focal thickening of the tunica intima and disruption of smooth muscle integrity, support aortic inflammation in the arsenic-exposed rats. ATV treatment in the arsenic-exposed rats brought the levels of the pro-inflammatory cytokines, chemokine, acute phase protein and cell adhesion molecules back to the control levels, demonstrating its vasculo-protective effect by suppression of inflammatory response. Further, ATV attenuated the arsenic-mediated aortic histological alterations. The reduction in the mononuclear cell infiltration with ATV may be ascribed to the decrease in the level of aortic MCP-1 (Zhou et al., 2008). Several mechanisms have been proposed for suppression of inflammatory response with ATV, including inhibition of ERK phosphorylation, IκBα degradation and COX-2 expression (Shao et al., 2012) as well as increase in expression of peroxisome proliferator-activator receptors, thereby increase in IκB level (NF-κB inhibitor) and inhibition of the Rho/Rho kinase activity (Kleemann et al., 2004; Nohria et al., 2008). However, based on the current observations, it may be deduced that the ATV-mediated improvement in the NO bioavailability could be a reason for restoration of the levels of the pro-inflammatory mediators and consequent mitigation of vascular inflammation.

## Conclusions

Subchronic exposure to arsenic through drinking water caused vascular dysfunction as evident by functional, biochemical and structural alterations in aorta. The dysfunction may relate to alterations in NO signaling and higher release of pro-inflammatory cytokines, which could exacerbate the production of cell adhesion molecules, acute phase protein and chemokine. ATV has the vasculo-protective potential to ameliorate arsenic-induced vascular dysfunction and inflammation by restoring acetylcholine-induced relaxation, normalizing NO signaling, production of pro-inflammatory mediators and cell adhesion molecules and improving aortic histology.

## Funding

This work was funded by the Department of Biotechnology (DBT), Ministry of Science and Technology, Government of India, New Delhi.

## Conflict of interest

The authors declare that there are no conflicts of interest.

## Acknowledgments

The Junior Research Fellowship (JRF) awarded to the first author by the Indian Council of Agricultural Research (ICAR), New Delhi, is gratefully acknowledged. The authors are thankful to the Director, Indian Veterinary Research Institute, for providing necessary facilities.

## References

Amarenco, P., Labreuche, J., 2009. Lipid management in the prevention of stroke: review and updated meta-analysis of statins for stroke prevention. Lancet Neurol. 8, 453–463.

Argos, M., Kalra, T., Rathouz, P.J., Chen, Y., Pierce, B., Parvez, F., Islam, T., Ahmed, A., Rakibuz-Zaman, M., Hasan, R., Sarwar, G., Slavkovich, V., Geen, A.V., Graziano, J., Ahsan, H., 2010. Arsenic exposure from drinking water, and all-cause and chronic-disease mortalities in Bangladesh (HEALS): a prospective cohort study. Lancet 376, 252–258.

Aung, P.P., Maxwell, H., Jepson, R.G., 2007. Lipid-lowering for peripheral arterial diseases of the lower limb. Cochrane Database Syst. Rev. 4, CD000123.

Bersot, T.P., 2011. Drug therapy for hypercholesterolemia and dyslipidemia. In: Brunton, L. L., Chabner, B.A., Knollmann, B.C. (Eds.), Goodman and Gilman's The Pharmacological Basis of Therapeutics. The Mc Grew Hill Company, pp. 877–908.

Biswas, D., Sen, G., Sarkar, A., Biswas, T., 2010. Atorvastatin acts synergistically with N-acetyl cysteine to provide therapeutic advantage against Fas-activated erythrocyte apoptosis during chronic arsenic exposure in rats. Toxicol. Appl. Pharmacol. http://dx.doi.org/10.1016/j.taap.2010.10.002.

Blake, G.J., Ridker, P.M., 2001. Novel clinical markers of vascular wall inflammation. Circ. Res. 89, 763–771.

Caliman, I.F., Lamas, A.Z., Dalpiaz, P.L.M., Medeiros, A.R.S., Abreu, G.R., Figueiredo, S.G., Gusmão, L.N., Andrade, T.U., Bissoli, N.S., 2013. Endothelial relaxation mechanisms and oxidative stress are restored by atorvastatin therapy in ovariectomized rats. PLoS One 8, e80892.

Chen, J., Kuhlencordt, P.J., Astern, J., Gyurko, R., Huang, P.L., 2001. Hypertension does not account for the accelerated atherosclerosis and development of aneurysms in male apolipoprotein e/endothelial nitric oxide synthase double knockout mice. Circulation 104, 2391–2394.

Chen, C.J., Wang, S.L., Chiou, J.M., Tseng, C.H., Chiou, H.Y., Hsueh, Y.M., Chen, S.Y., Wu, M.M., Lai, M.S., 2007. Arsenic and diabetes and hypertension in human populations: a review. Toxicol. Appl. Pharmacol. 222, 298–304.

Cheng, T.J., Chuu, J.J., Chang, C.Y., Tsai, W.C., Chen, K.J., Guo, H.R., 2011. Atherosclerosis induced by arsenic in drinking water in rats through altering lipid metabolism. Toxicol. Appl. Pharmacol. 256, 146–153.

Csanaky, I., Nemeti, B., Gregus, Z., 2003. Dose-dependent biotransformation of arsenite in rats — not S-adenosylmethionine depletion impairs arsenic methylation at high dose. Toxicology 183, 77–91.

Dimmeler, S., Fleming, I., Fisslthaler, B., Herman, C., Busse, R., Zeiher, A.M., 1999. Activation of nitric oxide synthase in endothelial cells by Akt-dependent phosphorylation. Nature 399, 601–605.

Fulton, D., Gratton, J.-P., Sessa, W.C., 2001. Post-translational control of endothelial nitric oxide synthase: why isn't calcium/calmodulin enough? J. Pharmacol. Exp. Ther. 299, 818–824.

Gragasin, F.S., Michelakis, E.D., Hogan, A., Moudgil, R., Hashimoto, K., Wu, X., Bonnet, S., Haromy, A., Archer, S.L., 2004. The neurovascular mechanism of clitoral erection: nitric oxide and cGMP-stimulated activation of $BK_{Ca}$ channels. FASEB J. 18, 1382–1391.

Guha Mazumder, D., Dasgupta, U.B., 2011. Chronic arsenic toxicity: studies in West Bengal, India. Kaohsiung J. Med. Sci. 27, 360–370.

Gurr, J.R., Yih, L.H., Samikkannu, T., Bau, D.T., Lin, S.Y., Jan, K.Y., 2003. Nitric oxide production by arsenite. Mutat. Res. 533, 173–182.

Huang, P.L., Huang, Z., Mashimo, H., Bloch, K.D., Moskowitz, M.A., Bevan, J.A., Fishman, M.C., 1995. Hypertension in mice lacking the gene for endothelial nitric oxide synthase. Nature 377, 239–242.

Janssen-Heininger, Y.M., Poynter, M.E., Baeuerle, P.A., 2000. Recent advances towards understanding redox mechanisms in the activation of nuclear factor κB. Free Radic. Biol. Med. 28, 1317–1327.

Jiang, J., Ashekuzzaman, S.M., Jiang, A., Sharifuzzaman, S.M., Chowdhury, S.R., 2013. Arsenic contaminated groundwater and its treatment options in Bangladesh. Int. J. Environ. Res. Public Health 10, 18–46.

Jindal, S., Singh, M., Balakumar, P., 2008. Effect of bis (maltolato) oxovanadium (BMOV) in uric acid and sodium arsenite-induced vascular endothelial dysfunction in rats. Int. J. Cardiol. 128, 283–291.

Kandasamy, K., Prawez, S., Choudhury, S., More, A.S., Ahanger, A.A., Singh, T.U., Parida, S., Mishra, S.K., 2011. Atorvastatin prevents vascular hyporeactivity to norepinephrine in sepsis: role of nitric oxide and $\alpha_1$-adrenoceptor mRNA expression. Shock 36, 76–82.

Kasper, H.U., Schmidt, A., Roessner, A., 1996. Expression of the adhesion molecules ICAM, VCAM, and ELAM in the arteriosclerotic plaque. Gen. Diagn. Pathol. 141, 289–294.

Kaur, T., Goel, R., Balakumar, P., 2010. Effect of rosiglitazone in sodium arsenite induced experimental vascular endothelial dysfunction. Arch. Pharm. Res. 33, 611–618.

Kawashima, S., Yokoyama, M., 2004. Dysfunction of endothelial nitric oxide synthase and atherosclerosis. Arterioscler. Thromb. Vasc. Biol. 24, 998–1005.

Kleemann, R., Verschuren, L., de Rooji, B., Lindeman, J., de Matt, M.M., Szalai, A.J., Princen, H. M.G., Kooistra, T., 2004. Evidence for anti-inflammatory activity of statins and PPARα activators in human C-reactive protein transgenic mice in vivo and in cultured human hepatocytes in vitro. Blood 103, 4188–4194.

Kumagai, Y., Pi, J., 2004. Molecular basis for arsenic-induced alteration in nitric oxide production and oxidative stress: implication of endothelial dysfunction. Toxicol. Appl. Pharmacol. 198, 450–457.

Lee, M.Y., Jung, B.I., Chung, S.M., Bae, O.N., Lee, J.Y., 2003. Arsenic-induced dysfunction in relaxation of blood vessels. Environ. Health. Perspect. 111, 513–517.

Li, H., Forstermann, U., 2009. Prevention of atherosclerosis by interference with the vascular nitric oxide system. Curr. Pharm. Des. 15, 3133–3145.

Liao, J.K., Laufs, U., 2005. Pleiotropic effects of statins. Annu. Rev. Pharmacol. Toxicol. 45, 89–118.

Livak, K.J., Schmittgen, T.D., 2001. Analysis of relative gene expression data using real-time quantitative PCR and the 29(−Delta Delta C(T)) method. Methods 25, 402–408.

Majhi, C.R., Khan, S., Leo, M.D.M., Manimaran, A., Sankar, P., Sarkar, S.N., 2011. Effects of acetaminophen on reactive oxygen species and nitric oxide redox signaling in kidney of arsenic-exposed rats. Food Chem. Toxicol. 49, 974–982.

Matthews, J.R., Botting, C.H., Panico, M., Morris, H.R., Hay, R.T., 1996. Inhibition of NF-κB DNA binding by nitric oxide. Nucleic Acids Res. 24, 2236–2242.

Niu, X.F., Smith, C.W., Kubes, P., 1994. Intracellular oxidative stress induced by nitric oxide synthesis inhibition increases endothelial cell adhesion to neutrophils. Circ. Res. 74, 1133–1140.

Nohria, A., Prsic, A., Liu, P.Y., Okamoto, R., Creager, M.A., Selwyn, A., Liao, J.K., Ganz, P., 2008. Statins inhibit Rho kinase activity in patients with atherosclerosis. Atherosclerosis 205, 517–521.
Paffen, E., deMaat, M.P.M., 2006. C-reactive protein in atherosclerosis: a causal factor? Cardiovasc. Res. 71, 30–39.
Papayianni, A., Alexopoulos, E., Giamalis, P., Gionanlis, L., Belechri, A.M., Koukoudis, P., Memmos, D., 2002. Circulating levels of ICAM-1, VCAM-1, and MCP-1 are increased in haemodialysis patients: association with inflammation, dyslipidaemia, and vascular events. Nephrol. Dial. Transplant. 17, 435–441.
Pi, J., Horiguchi, S., Sun, Y., Nikaido, M., Shimojo, N., Hayashi, T., Yamauchi, H., Itoh, K., Yamamoto, M., Sun, G., Waalkes, M.P., Kumagai, Y., 2003. A potential mechanism for the impairment of nitric oxide formation caused by prolonged oral exposure to arsenate in rabbits. Free Radic. Biol. Med. 35, 102–113.
Prabu, S.M., Muthumani, M., 2012. Silibinin ameliorates arsenic induced nephrotoxicity by abrogation of oxidative stress, inflammation and apoptosis in rats. Mol. Biol. Rep. 39, 11201–11216.
Rahaman, S., Sinha, A.C., Pati, R., Mukhopadhyay, D., 2013. Arsenic contamination: a potential hazard to the affected areas of West Bengal, India. Environ. Geochem. Health 35, 119–132.
Rang, H.P., Dale, M.M., Ritter, J.M., Flower, R.J., Henderson, G., 2012. Nitric oxide. Rang and Dale's Pharmacology. Elsevier, pp. 237–245 (Churchill Livingstone).
Rott, D., Zhu, J., Zhou, Y.F., Burnett, M.S., Zaalles-Ganley, A., Epstein, S.E., 2003. IL-6 is produced by spenocytes derived from CMV-infected mice in response to CMV antigens, and induces MCP-1 production by endothelial cells: a new mechanistic paradigm for infection-induced atherogenesis. Atherosclerosis 170, 223–228.
Roy, D., Das, T.K., Vaswani, S., 2013. Arsenic: its extent of pollution and toxicosis: an animal perspective. Vet. World 6, 53–58.
Savoia, C., Schiffrin, E.L., 2006. Inflammation in hypertension. Curr. Opin. Nephrol. Hypertens. 15, 152–158.
Scumpia, P.O., Sarcia, P.J., Demarco, V.G., Stevens, B.R., Skimming, J.W., 2002. Hypothermia attenuates iNOS, CAT-1, CAT-2 and nitric oxide expression in lungs of endotoxemic rats. Am. J. Physiol. 283, 1231–1238.
Shao, Q., Shen, L.H., Hu, L.H., Pu, J., Jing, Q., He, B., 2012. Atorvastatin suppresses inflammatory response induced by oxLDL through inhibition of ERK phosphorylation, IκBα degradation, and COX-2 expression in murine macrophages. J. Cell. Biochem. 113, 611–618.
Sharma, B., Sharma, P.M., 2013. Arsenic toxicity induced endothelial dysfunction and dementia: pharmacological interdiction by histone deacetylase and inducible nitric oxide synthase inhibitors. Toxicol. Appl. Pharmacol. 273, 180–188.
Simeonova, P.P., Hulderman, T., Harki, D., Luster, M.I., 2003. Arsenic exposure accelerates atherogenesis in Apolipoprotein E(−/−) mice. Environ. Health Perspect. 111, 1744–1748.
Springer, T.A., 1994. Traffic signals for lymphocyte recirculation and leukocyte emigration: the multistep paradigm. Cell 76, 301–314.
Srivastava, S., Vladykovskaya, E.N., Haberzettl, P., Sithu, S.D., D'Souza, S.E., States, J.C., 2009. Arsenic exacerbates atherosclerotic lesion formation and inflammation in ApoE −/− mice. Toxicol. Appl. Pharmacol. 241, 90–100.
States, J.C., Srivastava, S., Chen, Y., Barchowsky, A., 2009. Arsenic and cardiovascular disease. Toxicol. Sci. 107, 312–323.
Stea, F., Bianchi, F., Cori, L., Sicari, R., 2014. Cardiovascular effects of arsenic: clinical and epidemiological findings. Environ. Sci. Pollut. Res. 21, 244–251.
Steed, M.M., Tyagi, N., Sen, U., Schuschke, D.A., Joshua, I.G., Tyagi, S.C., 2010. Functional consequences of the collagen/elastin switch in vascular remodeling in hyperhomocysteinemic wild-type eNOS −/− and iNOS −/− mice. Am. J. Physiol. Lung Cell. Mol. Physiol. 299, L301–L311.
Styblo, M., Del Razo, L., Vega, L., Germolec, D.R., Le Cluyse, E.L., Hamilton, G.A., Reed, W., Wang, C., Cullen, W.R., Thomas, D.J., 2000. Comparative toxicity of trivalent and pentavalent inorganic and methylated arsenicals in rat and human cells. Arch. Toxicol. 74, 289–299.
Subramani, J., Kathirvel, K., Leo, M.D., Kuntamallappanavar, G., Singh, T.U., Mishra, S.K., 2009. Atorvastatin restores the impaired vascular endothelium-dependent relaxations mediated by nitric oxide and endothelium-derived hyperpolarizing factors but not hypotension in sepsis. J. Cardiovasc. Pharmacol. 54, 526–534.
Sumi, D., 2008. Biological effects of and responses to exposure to electrophilic environmental chemicals. J. Health Sci. 54, 267–272.
Sun, J., Druhan, L.J., Zweier, J.L., 2010. Reactive oxygen and nitrogen species regulate inducible nitric oxide synthase function shifting the balance of nitric oxide and superoxide production. Arch. Biochem. Biophys. 494, 130–137.
Szmitko, P.E., Wang, C.H., Weisel, R.D., de Almeida, J.R., Anderson, T.J., Verma, S., 2003. New markers of inflammation and endothelial cell activation: part I. Circulation 108, 1917–1923.
Tedder, T.F., Steeber, D.A., Chen, A., Engel, P., 1995. The selectins: vascular adhesion molecules. FASEB J. 9, 866–873.
Tsou, T., Tsai, F., Hsieh, Y., Li, L., Yeh, S.C., Chang, L.W., 2005. Arsenite induces endothelial cytotoxicity by down-regulation of vascular endothelial nitric oxide synthase. Toxicol. Appl. Pharmacol. 208, 277–284.
Verma, S., Reddy, K., Balakumar, P., 2010. The defensive effect of benfotiamine in sodium arsenite induced experimental vascular endothelial dysfunction. Biol. Trace Elem. Res. 137, 96–109.
Virdis, A., Ghiadoni, L., Giannarrelli, C., Taddei, S., 2010. Endothelial dysfunction and vascular disease in later life. Maturitas 67, 20–24.
Wagner, A.H., Schwabe, O., Hecker, M., 2002. Atorvastatin inhibition of cytokine-inducible nitric oxide synthase expression in native endothelial cells in situ. Br. J. Pharmacol. 136, 143–149.
Wang, J., Weigand, L., Wang, W., Sylvester, J.T., Shimoda, L.A., 2005. Chronic hypoxia inhibits $K_v$ channel gene expression in rat distal pulmonary artery. Am. J. Physiol. 288, 1049–1058.
Wayman, N.S., Ellis, B.L., Thiemermann, C., 2003. Simvastatin reduces infarct size in a model of acute myocardial ischaemia and reperfusion in the rat. Med. Sci. Monit. 9, 195–199.
Yang, H.T., Chou, H.J., Han, B.C., Huang, S.Y., 2007. Lifelong inorganic arsenic compounds consumption affected blood pressure in rats. Food Chem. Toxicol. 45, 2479–2487.
Yeh, E.T.H., 2004. CRP as a mediator of disease. Circulation 109 (II-11-II-14).
Zhang, X., Recchia, F.A., Bernstein, R., Xu, X., Nasjletti, A., Hintze, T.H., 1999. Kinin-mediated coronary nitric oxide production contributes to the therapeutic action of angiotensin-converting enzyme and neutral endopeptidase inhibitors and amlodipine in the treatment in heart failure. J. Pharmacol. Exp. Ther. 288, 742–751.
Zhou, M.S., Schuman, I.H., Jaimes, E.A., Raij, L., 2008. Renoprotection by statins is linked to a decrease in renal oxidative stress, TGF-β and fibronectin with concomitant increase in nitric oxide bioavailability. Am. J. Physiol. Renal Physiol. 295, F53–F59.